J|A|C|S
ARTICLES
Published on Web 02/08/2003

Isolation of the Latent Precursor Complex in Electron-Transfer Dynamics. Intermolecular Association and Self-Exchange with Acceptor Anion Radicals

Vellaichamy Ganesan, Sergiy V. Rosokha, and Jay K. Kochi*

Contribution from the Department of Chemistry, University of Houston, Houston, Texas, 77204

Received September 9, 2002; E-mail: jkochi@mail.uh.edu

Abstract: Transient [1:1] complexes formed in the bimolecular interactions of electron acceptors (**A**) with their reduced anion radicals ($\mathbf{A}^{-\bullet}$) are detected and characterized in solution for the first time. The recognition of such metastable intermediates as the heretofore elusive precursor complex ($\mathbf{A_2}^{-\bullet}$) in electron-transfer processes for self-exchange allows the principal parameters λ (Marcus reorganization energy) and H_{DA} (electronic coupling element) to be experimentally determined from the optical (charge-transfer) transitions inherent to these intermolecular complexes. The satisfactory correspondence of the theoretically predicted with the experimentally observed rate constants validates these ET parameters and the Marcus−Hush−Sutin methodology for strongly coupled redox systems lying in the (Robin-Day) Class II category. Most importantly, the marked intermolecular electronic interaction (H_{DA}) within these precursor complexes must be explicitly recognized, since it dramatically affects the electron-transfer dynamics by effectively lowering the activation barrier. As such, the numerous calculations of the reorganization energy previously obtained from various self-exchange kinetics based on $\lambda = 4\Delta G^*$ must be reconsidered in the light of such a precursor complex, with the important result that ET rates can be substantially faster than otherwise predicted. On the basis of these studies, a new mechanistic criterion is proposed for various outer-sphere/inner-sphere ET processes based on the relative magnitudes of H_{DA} and λ.

Introduction

The preequilibrium formation of the intermolecular [1:1] precursor or encounter complex between an electron donor (**D**) and an acceptor (**A**) is consistently included in the most general formulations of electron-transfer mechanisms,[1] i.e.,

$$\mathbf{D} + \mathbf{A} \rightleftarrows [\mathbf{D},\mathbf{A}] \rightleftarrows \mathbf{D}^+ + \mathbf{A}^- \qquad (1)$$

However, the importance of such metastable complexes [**D**,**A**] to the overall ET dynamics has been difficult to evaluate quantitatively owing to the limited number of experimental probes available for the detection of these elusive intermediates in solution.[2−4] As a result, most electron-transfer studies have heretofore simply classified them generically as outer-sphere complexes with rather small (invariant) formation constants that by and large leave the dynamics unaffected.[1,5−7]

To demonstrate quantitatively how the precursor complex (PC) plays a critical role in electron-transfer dynamics, we now focus on the redox behavior of the prototypical (organic) acceptors (**A**) illustrated in Chart 1 for three principal reasons: (a) they are all planar π-acceptors with reversible redox potentials in a reasonable E^0_{red} range, (b) the reduced anion radicals ($\mathbf{A}^{-\bullet}$) are stable in solution and can be rigorously

Chart 1

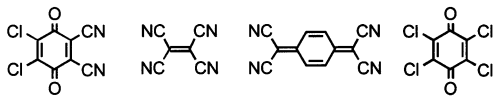

	DDQ	TCNE	TCNQ	CA
E^o_{red} (V *vs.* SCE)	0.52	0.24	0.19	-0.02

(1) (a) Sutin, N. *Prog. Inorg. Chem.* **1983**, *30*, 441. (b) Note that in self-exchange the successor complex is equivalent to the precursor complex denoted in generalized electron-transfer formulations.
(2) For a trenchant evaluation of the precursor complexes in intermolecular organic electron transfer, see: Nelsen, S.; Pladziewicz, J. *Acc. Chem. Res.* **2002**, *35*, 247.
(3) For the spectral characterization of precursor complexes in the outer-sphere electron transfer of coordination compounds, see: (a) Khoshtariya, D. E.; Meusinger, R.; Billing, R. *J. Phys. Chem.* **1995**, *99* (9), 3592. (b) Curtis, J. C.; Sullivan, B. P.; Meyer, T. J. *Inorg. Chem.* **1980**, *19*, 3833.
(4) For the analysis of intramolecular thermal/optical electron transfer in bridged mixed-valence systems as prototypes for the precursor complex in intermolecular electron transfer, see: (a) Elliot, C. M.; Derr, D. L.; Matyushov, D. V.; Newton, M. D. *J. Am. Chem. Soc.* **1998**, *120*, 11714. (b) Nelsen, S. F.; Adamus, J.; Wolff, J. J. *J. Am. Chem. Soc.* **1994**, *116*, 1589. (c) Nelsen, S. F.; Ramm, M. T.; Wolff, J. J.; Powell, D. R. *J. Am. Chem. Soc.* **1997**, *119*, 6863. (d) Nelsen, S. F.; Trieber, D. A.; Wolff, J. J.; Powell, D. R.; Rogers-Crowley S. *J. Am. Chem. Soc.* **1997**, *119*, 6873. (e) Nelsen, S. F.; Ismagilov, R. F.; Powell, D. R. *J. Am. Chem. Soc.* **1997**, *119*, 10213. (f) Lindeman, S. V.; Rosokha, S. V.; Sun, D.; Kochi, J. K. *J. Am. Chem. Soc.* **2002**, *124*, 843. (g) Kambhampati, P.; Son, D. H.; Kee, T. W.; Barbara, P. F. *J. Phys. Chem. A* **2000**, *104*, 10637. (h) Son, D. H.; Kambhampati, P.; Kee, T. W.; Barbara, P. F. *J. Phys. Chem. A* **2002**, *106*, 4591.
(5) (a) Marcus, R. A. *Angew. Chem., Int. Ed. Engl.* **1993**, *32*, 1111. (b) Marcus, R. A. *Discuss. Faraday Soc.* **1960**, *29*, 21. (c) Marcus, R. A. *J. Phys. Chem.* **1963**, *67*, 853. (d) Marcus, R. A. *J. Chem. Phys.* **1965**, *43*, 679. (e) Marcus, R. A.; Sutin, N. *Biochim. Biophys. Acta* **1985**, *811*, 265.
(6) (a) Astruc, D. *Electron Transfer and Radical Processes in Transition-Metal Chemistry*; VCH: New York, 1995. (b) Eberson, L. *Electron-Transfer Reactions in Organic Chemistry;* Springer-Verlag: New York, 1987. (c) Cannon, R. D. *Electron-Transfer Reactions*; Butterworth: London, 1980. (d) Formosinho, S. J.; Arnaut, L. G.; Fausto, R. *Prog. React. Kinet.* **1998**, *23*, 1.

characterized via isolation as pure crystalline salts, and (c) their electron-transfer rates are relatively fast and experimentally accessible.[8] These electron acceptors, particularly TCNQ and TCNE, have also been recently utilized in the discovery and development of molecule-based (semi)conductors and magnets of importance to the burgeoning field of organic materials science.[9]

For the electron acceptors in Chart 1, we directly address the simplest electron-transfer system that occurs in the absence of any driving-force contribution ($\Delta G^0_{ET} = 0$), namely, the detailed energy profile for the self-exchange (SE) dynamics, as typically indicated for tetracyanoethylene in eq 2. As such, the

$$\mathrm{TCNE} + \mathrm{TCNE}^{-\bullet} \overset{K_{SE}}{\rightleftharpoons} \mathrm{TCNE}^{-\bullet} + \mathrm{TCNE} \qquad (2)$$

presence of the precursor complex can be unambiguously assigned to the intermolecular association of the TCNE with its reduced anion radical to form the pertinent (preequilibrium) intermediate, i.e.,

$$\mathrm{TCNE} + \mathrm{TCNE}^{-\bullet} \overset{K_{PC}}{\rightleftharpoons} [\mathrm{TCNE,TCNE}^{-\bullet}] \qquad (3)$$

Although these dimeric anion-radical complexes in solution are unreported, the possibility of such an association can be seen in the extant solid-state data.[10]There are also a few examples of a somewhat related [1:1] self-association comprised of aromatic donors (ArH) complexed with their own cation radicals, i.e., $(ArH)_2^{+\bullet}$.[11] Most importantly, these unusual (intermolecular) complexes are spectrally characterized by diagnostic absorption bands in the near-infrared (NIR) region[11] that have been shown to arise from the charge-transfer or CT interaction of the aromatic hydrocarbon acting as the electron donor with its positively charged cation radical as the acceptor.[12]The extension of the same Mulliken formulation[13] to the electron-poor π-acceptors in Chart l leads to negatively charged CT complexes, with the relatively electron-rich anion radicals acting as the π-donors. Accordingly, our primary task lies in the unambiguous identification and spectral characterization of the corresponding anion-radical π-mers $(\mathbf{A_2})^{-\bullet}$ for the electron acceptors in Chart l.[11] We then establish how these precursor complexes lead to the mapping out of the energy profile and to new insights into the electron-transfer mechanism of the self-exchange process, i.e.,

$$\mathbf{A} + \mathbf{A}^{-\bullet} \rightleftarrows [\mathbf{A_2}^{-\bullet}] \rightleftarrows \mathbf{A}^{-\bullet} + \mathbf{A}$$

Results

I. Isolation and X-ray Crystallography of Anion-Radical Salts. The polycyano alkenes (TCNE and TCNQ) and the quinones (DDQ and CA) were sufficiently electron deficient to effect the one-electron oxidation of iodide for the preparation of crystalline alkali-metal and alkylammonium salts [see Experimental Section]. Analysis of the X-ray crystallographic data indicated that one-electron reductions of π-acceptors resulted in substantial (selective) changes of the bond lengths, and the characteristic structural changes in these acceptors upon their reduction to the corresponding anion radicals are presented in Chart 2.[14] [For the complete structural parameters of the neutral donors and their anion radicals, see Table S1 in the Supporting Information.]

X-ray crystallographic studies indicated that the characteristic feature of π-anion radicals was their tendency for intermolecular

(7) For kinetic studies of electron-transfer self-exchange, see: (a) Jurgen, D.; Pedersen, S.; Pedersen, J. A.; Lund, H. *Acta Chem. Scand.* **1997**, *51*, 767. (b) Larsen, H.; Pedersen, S. U.; Pedersen, J. A.; Lund, H. *J. Electroanal. Chem.* **1992**, *331*, 971. (c) Fukuzumi, S.; Nakanishi, I.; Suenobu, T.; Kadish, K. M. *J. Am. Chem. Soc.* **1999**, *121*, 3468. (d) Grampp, G.; Rauhut, G. *J. Phys. Chem.* **1995**, *99*, 1815. (e) Grampp, G.; Jaenicke, W. *J. Chem. Soc., Faraday Trans. 2* **1985**, 81,1035. (f) Nelsen, S. F.; Blackstock, S. C. *J. Am. Chem. Soc.* **1985**, *107*, 7189. (g) Malinovski, G. L., Jr.; Bruning, W. H.; Griffin, R. G. *J. Am. Chem. Soc.* **1970**, *92*, 2665. (h) Ward, R. L.; Weissman, S. I. *J. Am. Chem. Soc.* **1957**, *79*, 2086. (i) Haran, N.; Luz, Z.; Shporer, M. *J. Am. Chem. Soc.* **1974**, *119*, 6873. For theoretical (quantum-mechanical) studies of self-exchange, see: (j) Jacobsen, S.; Mikkelsen, K. V.; Pedersen, S. U. *J. Phys. Chem.* **1996**, *100*, 7411. (k) Mikkelsen, K. V.; Pedersen, S. U.; Lund, H.; Swanstrøm, P. *J. Phys. Chem.* **1991**, *95*, 8892. (l) Ma, S.-H.; Zhang, X.-D.; Xu, H.; Shen, L.-L.; Zhang, X.-K.; Zhang, Q.-Y. *J. Photochem. Photobiol. A: Chem.* **2001**, *139*, 97. (m) Kelterer, A.-M.; Landgraf, S.; Grampp, G. *Spectrochim. Acta* **2001**, *A57*, 1959. (n) Vener, M. V.; Ioffe, N. T.; Cheprakov, A. V.; Mairanovsky, V. G. *J. Electroanal. Chem.* **1994**, *370*, 33. (o) Rauhut, G.; Clark, T. *J. Am. Chem. Soc.* **1993**, *115*, 9127.

(8) For kinetic measurements of electron-transfer self-exchange processes with DDQ, TCNQ, and TCNE, see: (a) Komarynsky, M. A.; Wahl A. C. *J. Phys. Chem.* **1975**, *79*, 695. (b) Phillips, W. D.; Rowell, J. C.; Weissman, S. I *J. Chem. Phys.* **1960**, *33*, 626. (c) Watts, M. T.; Lu, M. L.; Chen, R. C.; Eastman, M. P *J. Phys. Chem.* **1973**, *77*, 2959. (d) Ogasawara, M.; Takaoka, H.; Hayashi, K. *Bull. Chem. Soc. Jpn.* **1973**, *46*, 35. (e) Grampp, G.; Landgraf, S.; Rasmussen, K. *J. Chem. Soc., Perkin Trans. 2* **1999**, 1897. (f) Grampp, G.; Jaenicke, W. *Ber. Bunsen-Ges. Phys. Chem.* **1991**, *95*, 904. (g) Grampp, G.; Harrer, W.; Hetz, G. *Ber. Bunsen-Ges. Phys. Chem.* **1990**, *94*, 1343. (h) Grampp, G. *Spectrochim. Acta* **1998**, *A54*, 2349.

(9) (a) Miller, J. S. *Inorg. Chem.* **2000**, *39*, 4392. (b) Williams, J. M. *Organic Superconductors* (*Including Fullerenes*): *Synthesis, Structure, Properties and Theory*; Prentice Hall: Englewood Cliffs, NJ, 1992. (c) Ferraro, J. R.; Williams, J. M. *Introduction to Synthetic Electrical Conductors*; Academic Press: Orlando, 1987.

(10) (a) There are, however, some solid-state data[10b,c,17,19] of anion-radical associates with their parent acceptors (π-mer) that are characterized by NIR absorption bands, which are similar to the charge-resonance absorption invariably found as a common (diagnostic) feature of cation-radical associates.[11,12] However, the available data did not prove the (noticeable) association of the free anion radical with its neutral parent in solution,[10d] nor allow the determination of the corresponding extinction coefficients and formation constants. (b) The NIR charge-resonance transition in the anthracene π-mer $(\mathbf{A_2})^{-\bullet}$ was observed after the irradiation of dianthracene in a rigid MTHF matrix, see: Shida, T.; Iwata, S. *J. Chem. Phys.* **1972**, *56*, 2858. (c) The NIR absorption band was observed in the solid-state spectrum of $(TCNQ_2)^-$. See: Terashita, S.; Nacatsu, K.; Ozaki, Y.; Takagi, S. *J. Phys. Chem.* **1995**, *99*, 3618. (d) For ESR spectroscopic indications of the presence of (tetrafluorobenzene and octafluoronaphthalene) anion-radical π-mers in hexane, see: Werst, D. W. *Chem. Phys. Lett.* **1993**, *202*, 101; *Chem. Phys. Lett.* **1996**, *251*, 315.

(11) (a) Lewis, L. C.; Singer, L. S. *Chem. Phys*. **1965**, *43*, 2712. (b) Howarth, O. W.; Fraenkel, G. K. *J. Am. Chem. Soc.* **1966**, *88*, 4514. (c) Howarth, O. W.; Fraenkel, G. K. *J. Chem. Phys*. **1970**, *52*, 6258. (d) Badger, B.; Brocklehurst, B. *Nature* **1968**, *219*, 263. (d) Badger, B.; Brocklehurst, B.; Dudley, R. *Chem. Phys. Lett.* **1967**, *1*, 122. (e) Badger, B.; Brocklehurst, B. *Trans. Faraday Soc.* **1969**, *65*, 2582. (f) Badger, B.; Brocklehurst, B. *Trans. Faraday Soc.* **1969**, *65*, 2588. (g) Badger, B.; Brocklehurst, B. *Trans. Faraday Soc.* **1970**, *66*, 2939. (h) Meot-Ner, M.; Hamlet, P.; Hunter, E. P.; Field, F. H. *J. Am. Chem. Soc.* **1978**, *100*, 5466. (i) Meot-Ner, M. *J. Phys. Chem.* **1980**, *84*, 2724. (j) Meot-Ner, M.; El-Shall, M. S. *J. Am. Chem. Soc.* **1986**, *108*, 4386. (k) All attempts to prepare the corresponding *anionic* dimers in solution were unsuccessful heretofore. (l) Since the cationic and anionic dimers are both derived from π-donor/acceptor pairs, they are hereinafter referred to (generically) as "π-mers" or precursor complexes, interchangeably. [The designation "dimer" is reserved for the dianionic $(\mathbf{A_2})^{2-}$ complex.[15,18]]

(12) For the spectral and structural characterization of such cation-radical "π-mers", see: (a) Le Magueres, P.; Lindeman, S.; Kochi, J. K. *J. Chem. Soc., Perkin Trans. 2* **2001**, 1180. (b) Kochi, J. K.; Rathore, R.; Le Magueres, P. *J. Org. Chem.* **2000**, *65*, 6826, and references therein.

(13) (a) Mulliken, R. S. *J. Am. Chem. Soc.* **1952**, *74*, 811. (b) Mulliken, R. S.; Person, W. B. *Molecular Complexes*; Wiley: New York, 1969.

(14) (a) The numbers besides the bonds in Chart 2 represent the average differences (in 10^{-1} pm) between the (corresponding) bond length in the anion radical and its parent acceptor (the "+" sign indicates a longer bond in the reduced species). Note, for clarity, only changes in one of the symmetrically equivalent bonds are shown (see Table S1, Supporting Information, for scatter of the data). The data used are from measurements made in this study, as well as those taken from: (b) Miller, J. S.; Krusic, P. J.; Dixon, D. A.; Reiff, W. M.; Zhang, J. H.; Anderson, E. C.; Epstein, A. J. *J. Am. Chem. Soc.* **1986**, *108*, 4459. (c) Miller, J. S.; Zhang, J. H.; Reiff, W. M.; Dixon, D. A.; Preston, L. D.; Reis, A. H., Jr.; Gebert, E.; Extine, M.; Troup, J.; Epstein, A. J.; Ward, M. D. *J. Phys. Chem.* **1987**, *91*, 4344. (d) Dixon, D. A.; Miller, J. S. *J. Am. Chem. Soc.* **1987**, *109*, 3656, and references therein.

Chart 2

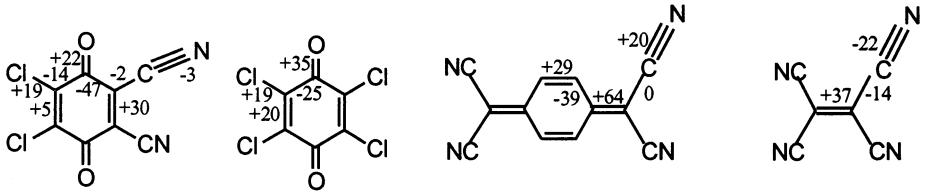

association. One form of such an association (found for all these acceptors) was the self-formation of diamagnetic (dianionic) dimers,[15]in which a pair of anion radicals were characterized by face-to-face arrangement of planar moieties, and the interplanar distances were substantially less than the sum of the corresponding van der Waals radii. The other form of association (of particular interest here) included the interaction of various electron acceptors with their corresponding anion radicals. For example, when the crystallization of TCNQ was carried out in the presence of its anion radical, mixed crystals were found with stoichiometric 1:1, 2:1, and 3:2 ratios of TCNQ relative to $TCNQ^{-\bullet}$.[16]The paramagnetic $(TCNQ)_2^{-\bullet}$ dyad could be clearly recognized in these crystals as two acceptor moieties sharing one electron.[17]The cofacial arrangement in such associations (similar to those in the dimers) occurred with an interplanar separation (3.2−3.3 Å) that was much less than the sum of van der Waals radii[17] to indicate a substantial intermolecular interaction between the counterparts. The structural parameters of both components within such a dyad were indistinguishable, with bond lengths that were intermediate between those characteristic of the neutral acceptor and those of the anion radical.

Crystallization from solution of a mixture of $DDQ^{-\bullet}$ and DDQ also resulted in the formation of the mixed complexes (see Experimental Section). The molar ratio of the anion radical to the neutral acceptor in such crystals was 2:1, but the partial (crystal) disorder precluded a precise analysis of the individual bond lengths within each moiety. Nonetheless, the cofacial arrangement of all three moieties with an interplanar distance substantially less than the sum of van der Waals radii can be clearly recognized in Figure 1. In the case of TCNE and CA, our numerous efforts to obtain crystalline associates between the neutral acceptor and its anion radical always resulted in mixed crystals consisting of the separate neutral acceptor and the separate anion-radical salt. [The latter was in the form of either the anion-radical salt itself or its dianionic dimer.]

II. Spectral Characterization and Analysis of the Precursor Complexes. The electron acceptors **A** in Chart 1 were characterized in solution by prominent (UV−vis) absorption bands at 330 ± 70 nm ($\epsilon_{max} \approx 10^4$ M^{-1} cm^{-1}), as listed in Table 1. One-electron reduction to their anion radicals $\mathbf{A}^{-\bullet}$ was accompanied by the appearance of additional strong absorption bands in the visible region between 420 and 850 nm ($\epsilon_{max} \approx 10^4$ M^{-1} cm^{-1}). The UV−vis spectra of the neutral acceptors as well as their anion radicals showed little solvent dependence ($\Delta\lambda < 500$ cm^{-1}) in dichloromethane (apolar) and acetonitrile (polar) solutions, and the change in the cationic counterion from sodium to tetrabutylammonium did not materially affect the electronic spectra (Table S2 in Supporting Information.)[18] Most important was the fact that no absorption bands were observed in the near-IR region even at high concentrations and low temperatures, provided solutions of the pure π-acceptor and its anion radical were examined separately. On the other hand,

Table 1. Spectral Characteristics of the Anion-Radical Dimers, $(A_2)^{-\bullet}$, in Comparison with Those of Their Neutral Parent Acceptor, **A**, and Anion Radicals, $\mathbf{A}^{-\bullet}$, as Well as the Formation Constants, K_a, of the Precursor Complex $(\mathbf{A_2})^{-\bullet}$[a]

	spectral characteristics, λ, nm (ϵ, 10^3 M^{-1} cm^{-1})			
acceptor	**A**	$\mathbf{A}^{-\bullet}$[b]	$(\mathbf{A}_2)^{-\bullet}$	K_{PC}, M^{-1}
DDQ	280 (27) 372 (0.8)	588 (6.3)	1370 (1.6)	3
TCNQ	396 (67)	842 (43)	2200 (3.2)	5
TCNE	270 (15)	428 (8.4)	1380 (1.0)	0.6
CA	287 (23) 367 (0.25)	449 (9.0)	1355(1.3)	4

[a] In acetonitrile, at 22 °C. [b] The characteristics of only the most intense band is presented. (For the other spectral bands, see Table S2 in the Supporting Information.)

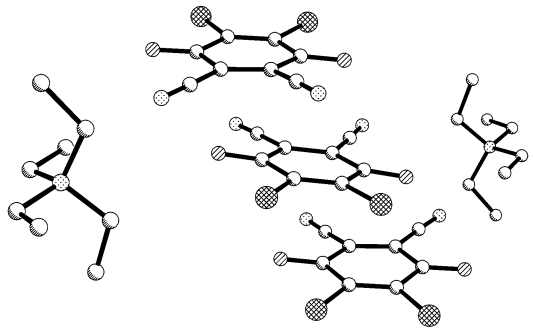

Figure 1. Molecular structure of $(Et_4N^+)_2(DDQ)_3^{2-}$ (hydrogen atoms are omitted for clarity). [Note that the mean interplanar separation between $DDQ/DDQ^{-\bullet}$ moieties is 2.90 Å compared to the sum (3.4 Å) of the van der Waals radii.]

(15) For the crystal structures of dimers, see e.g.: (a) DDQ: Yan, Y.-K.; Mingos, M. P.; Muller, T. E.; Williams, T. E.; Kurmoo, M. *J. Chem. Soc., Dalton Trans.* **1995**, 2509. (b) TCNE: Novoa, J. J.; Lafuente, P.; Del Seto, R. E.; Miller, J. S. *Angew. Chem., Int. Ed.* **2001**, *40*, 2540. (c) TCNQ: Grossel, M. C.; Weston, S. C. *Chem. Mater.* **1996**, *8*, 977.

(16) (a) Harms, R.; Keller, H. J.; Nothe, D.; Wene, D. *Acta Crystallogr.* **1982**, *B38*, 2838. (b) Bigoli, F.; Deplano, P.; Devillanova, F. A.; Girlando, A.; Lippolis, V.; Mercuri, M.-L.; Pellinghelli, M.-A.; Trogu, E. F. *J. Mater. Chem.* **1998**, *8*, 1145. (c) Bigoli, F.; Deplano, P.; Devillanova, F. A.; Girlando, A.; Lippolis, V.; Mercuri, M.-L.; Pellinghelli, M.-A.; Trogu, E. F. *Inorg. Chem.* **1996**, *35*, 5403.

(17) (a) Goldstein, P.; Seff, K.; Trueblood, K. N. *Acta Crystallogr.* **1968**, *B24*, 778. (b) Hanson, A. W. *Acta Crystallogr.* **1968**, *B24*, 773. (c) Kobayashi, H. *Bull. Chem. Soc. Jpn.* **1974**, *47*, 1346. (d) Fourmigue, M.; Perrocheau, V.; Clerac, R.; Coulon, C. *J. Mater. Chem.* **1997**, *7*, 2235. Ballester, L.; Gutierrez, A.; Perpinan, M. F.; Rico, S.; Azcondo, M. T.; Bellito, C. *Inorg. Chem.* **1999**, *38*, 4430.

(18) (a) It should be noted that anion radicals form dimers $(\mathbf{A}_2)^{2-}$ in the solid state,[15] and in solution this process is noticeable at high concentrations of anion radicals, especially in polar solvents at low temperatures. The dimers are characterized by absorption bands in the visible region, and these are blue-shifted by 100−200 nm relative to the corresponding bands of monomeric anion radicals. Thus, $(DDQ_2)^{2-}$ is characterized by the band at 710 nm (ϵ = 6300) in acetonitrile, and similar bands in DMF, acetone, THF, EtOH, and H_2O.[18b] The $(TCNQ_2)^{2-}$ dimer is characterized (in H_2O) by bands at 370, 640, and 870 nm.[18c] The $(TCNE_2)^{2-}$ dimer has a band at 525 nm in ethanol and at 540 nm in MTHF. The $(CA_2)^{2-}$ dimer is characterized by the band at 550 nm in THF[18e] and at 380 and 670 nm in EtOH.[18f] (b) Yamagishi, A. *Bull. Chem. Soc. Jpn.* **1975**, *48*, 2440. (c) Bieber, A.; Andre, J. J. *Chem. Phys.* **1975**, *7*, 137. (d) Matsuzaki, S.; Mitsuishi, T.; Toyoda, K. *Chem. Phys Lett.* **1982**, *91*, 296. (e) Andre, J. J.; Will, G. *Chem. Phys Lett.* **1971**, *9*, 27. (f) Bieber, A.; Andre, J. J. *Chem. Phys.* **1975**, *7*, 137.

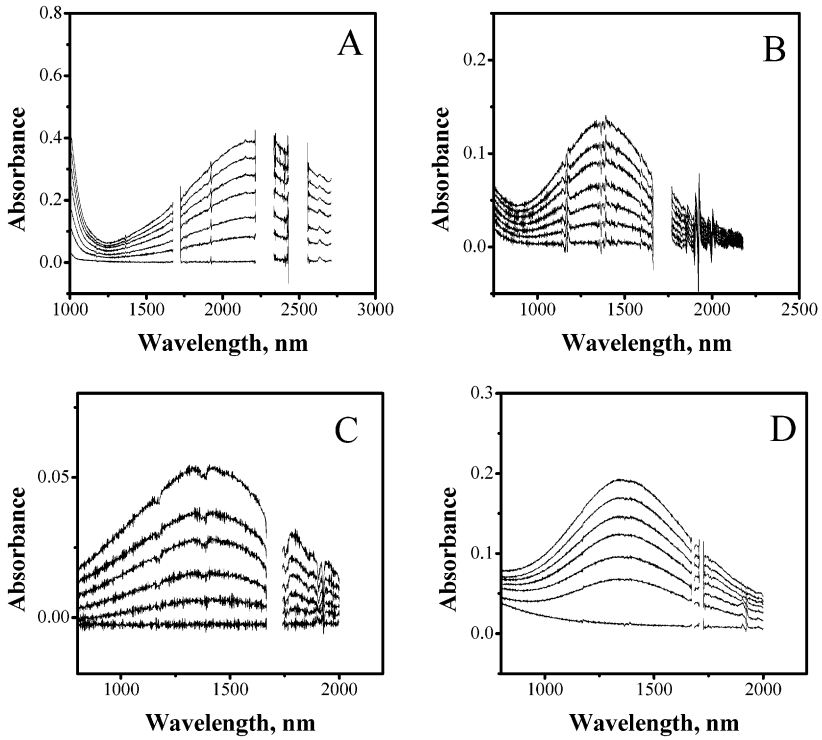

Figure 2. Spectral changes in the NIR region attendant upon incremental addition of parent acceptor molecule to the acetonitrile solution of the tetrabutylammonium salt of the corresponding anion radical: (A) 1.9 mM solution of $Bu_4N^+TCNQ^{-\bullet}$; concentration of neutral TCNQ (spectra from bottom to top): 0, 2.5, 4.4, 7.0, 8.8, 10.7, 12.5 mM; (B) 1.0 mM solution of $Bu_4N^+DDQ^{-\bullet}$; concentration of neutral DDQ (spectra from bottom to top): 0, 3.9, 7.8, 11.6, 16.4, 20.0, 24.4 mM; (C) 1.0 mM solution of $Bu_4N^+TCNE^{-\bullet}$; concentration of neutral TCNE (spectra from bottom to top): 0, 14, 33, 53, 72, 91 mM; (D) 2 mM solution of $Bu_4N^+CA^{-\bullet}$; concentration of neutral CA (spectra from bottom to top): 0, 6, 9, 12, 15, 18, 21 mM.

when *mixtures* of the neutral acceptor and its anion radical were examined, very weak absorption bands were observed in the NIR region. For example, the solution of pure $TCNQ^{-\bullet}$ in acetonitrile was characterized by the diagnostic absorption band at 842 nm. The stepwise addition of the parent TCNQ expectedly resulted in the appearance and growth of the 396 nm absorption and led to some spectral distortion of the absorption band of $TCNQ^{-\bullet}$ with concomitant diminution of the absorbance (see Figure S1 in the Supporting Information). However, careful scrutiny clearly revealed the additional appearance of a weak (broad) absorption in the NIR region at $\lambda_{max} = 2200$ nm, which progressively grew in intensity with further additions of TCNQ, as illustrated in Figure 2. Lowering the temperature of the TCNQ/$TCNQ^{-\bullet}$ solutions consistently led to substantial increases in only the new NIR absorbance.

To examine whether the counterion affected the NIR spectral changes, neutral TCNQ was incrementally added to acetonitrile solutions of $TCNQ^{-\bullet}$ successively taken as the lithium, sodium, and tetrabutylammonium salts. In all cases, the position of the NIR band was unchanged (see Figure S2 in the Supporting Information), and these measurements occurred with the same absorbance increase observed upon the further additions of $TCNQ^{-\bullet}$. Furthermore, the addition of TCNQ to its anion radical (taken as tetrabutylammonium salt) in other solvents such as dichloromethane and acetone also resulted in the appearance of similar NIR bands (see Table S2 in the Supporting Information). For example, in dichloromethane the affected NIR band at $\lambda_{max} = 2400$ nm corresponded to a slight shift of only 200 nm relative to that observed in the more polar acetonitrile.

These spectral observations, together with their similarity to the solid-state (reflectance) spectrum of various anionic π-mer salts of $(TCNQ)_2^{-\bullet}$,[19] were consistent with the dynamic association of the electron acceptor with its anion radical in solution, i.e.,

$$TCNQ + TCNQ^{-\bullet} \overset{K_{PC}}{\rightleftharpoons} (TCNQ)_2^{-\bullet} \qquad (4)$$

Indeed, the quantitative analysis of the equilibrium in eq 4 was successfully carried out by the Benesi-Hildebrand procedure,[20] i.e.,

$$[TCNQ^{-\bullet}]/A_{PC} = 1/\epsilon_{PC} + 1/(K_{PC}\epsilon_{PC}[TCNQ])$$

where A_{PC} was the absorbance and ϵ_{PC} was the molar extinction coefficient of the NIR band of the precursor complex at the monitoring wavelength, and $[TCNQ^{-\bullet}]$ and [TCNQ] were the initial concentrations of the anion radical and the parent, respectively. The plot of $[TCNQ^{-\bullet}]/A_{pc}$ versus reciprocal concentration of added TCNQ was linear, and the least-squares fit produced a correlation coefficient of greater than 0.99. The values of the association constant ($K_{PC} = 5\ M^{-1}$) and extinction coefficient ($\epsilon_{PC} = 3200\ M^{-1}cm^{-1}$) were obtained from the slope and the intercept (see Experimental Section).

The spectral behavior of the other electron acceptors in Chart 1 toward their corresponding anion radicals mirrored that of TCNQ. In each case, the appearance of a new absorption band in the NIR region (Table 1) signaled the formation of the intermolecular [1:1] precursor complex. Thus, the addition of

(19) Indication of the NIR band in solid-state salts containing $(TCNQ_2)^-$ is seen also from the data reported by: (a) Iida, Y. *Bull. Chem. Soc. Jpn.* **1969**, *42*, 637. (b) Tanaka, J.; Tanaka, M.; Kawai, T.; Takabe, T.; Maki, O. *Bull. Chem. Soc. Jpn.* **1976**, *49*, 2358.
(20) Benesi, H. A.; Hildebrand, J. H. *J. Am. Chem. Soc.* **1949**, *71*, 2703.

the quinone acceptor DDQ to an acetonitrile solution of its anion radical resulted in a new NIR band at $\lambda_{max} = 1360$ nm (Figure 2B and Figure S1 in the Supporting Information). Similar bands were obtained with the tetracyanoethylene and chloranil pairs, TCNE/TCNE$^{-\bullet}$ and CA/CA$^{-\bullet}$ in Figure 2C and D, respectively. For each dyad, the position of the corresponding NIR band and its intensity (at the same concentration) did not depend on whether sodium or tetrabutylammonium was the counterion (see Figure S2 in the Supporting Information), and this accords with previous observations[21] that these anion radicals exist largely in (polar) acetonitrile as free (separate) ions. Similar to TCNQ, the NIR bands also appeared upon the addition of neutral π-acceptors to their anion radicals in the other solvents. Thus in acetone, the positions of the NIR bands were close to those in acetonitrile, while in dichloromethane a slight (consistent) red-shift of the NIR band was observed (see Table S2 in the Supporting Information). Owing to the very low solubility of alkali metal salts of anion radicals in dichloromethane, only the π-mer formation of the tetrabutylammonium salt could be studied, but the use of the bulky counterion limited the ion-pairing effects. Finally, the small magnitudes of the formation constants K_{PC} in Table 1 indicated that the precursor complexes were to be uniformly classified as weak.

III. Intermolecular Associations of Electron Acceptors with Their Anion Radicals as Charge-Transfer Interactions. The spontaneous association of electron acceptors with their anion radicals as listed in Table 1 was highly reminiscent of the behavior of other well-known electron donor/acceptor dyads, especially when the relatively electron-rich anion radical ($\mathbf{A}^{-\bullet}$) was viewed as an electron donor. According to this analogy, the characteristic NIR absorption bands in Figure 2 should bear a direct relationship to the absorption bands previously associated with the charge-transfer complexes of the same acceptors with other types of electron-rich donors.[22]Indeed, such [1:1] electron donor/acceptor complexes of DDQ, TCNQ, TCNE, and CA were formed with the various types of aromatic donors listed in Table 2.[23]In this way, the NIR absorption bands of the precursor complexes in Figure 3 were related directly to the charge-transfer absorption bands in Table 2, the spectroscopic transition energies (ν_{CT}) of which followed the Mulliken relationship,[13] i.e.,

$$h\nu_{CT} = a(E^0_{ox} - E^0_{red}) + \text{constant}$$

where E^0_{red} is the reversible reduction potential of the electron acceptor (DDQ, TCNQ, TCNE, and CA), E^0_{ox} is the oxidation potential of the aromatic donor, and a is a constant as illustrated in Figure 3A−D. The unique point for the precursor complex at the origin (abscissa) of each of these plots was defined by the value at the intercept of $E_{ox} - E_{red} = 0$ since both reversible electrode potentials for this anion-radical π-mer ($\mathbf{A_2}^{-\bullet}$) are identical.

Table 2. Energy of the Charge-Transfer Transition for the Intermolecular Complexes of the Acceptors in Chart 1 with Different Organic Donors[a]

	donor	E^0_{ox}, V[b]	energy of the charge-transfer transition, eV: acceptor TCNQ	DDQ[c]	TCNE[d]	CA
1	benzene	2.62		3.05	3.19	
2	toluene	2.25		2.82	2.99	
3	*o*-xylene	2.16		2.62	2.82	3.03
4	*p*-xylene	2.01		2.43	2.65	
5	mesitylene	2.11		2.43	2.64	2.87
6	durene	1.84		2.13	2.38	2.61
7	pentamethylbenzene	1.71	2.32	2.08		2.53
8	hexamethylbenzene	1.62	2.10[e]	1.98	2.27	2.39[e]
9	hexaethylbenmzene	1.59			2.24	
10	naphthalene	1.54	2.30[e]	2.01	2.58	2.58[e]
11	anthracene	1.09	1.62			1.97
12	ethylbenzene	2.27			3.01	
13	cumene	2.29			2.97	
14	fluorene	1.55[f]		1.99		
15	2,6-dimethylnaphthalene	1.36[f]	2.00			2.32
16	biphenylene	1.30[f]		1.7	1.81	
17	pyrene	1.16	1.68	1.55	1.70	2.03
18	2,5-dimethyl-*p*-dimethoxybenzene	1.15[g]		1.7	1.94	
19	9-methylanthracene	0.96[f]	1.49		0.99	1.83
20	9,10-dimethylanthracene	0.94[f]	1.38			1.69
21	perylene	0.85	1.35			1.69
22	octamethylbiphenylene	0.80[d]	1.43[d]	1.41	1.41	1.51[d]
	π-mer		0.52 (0.56)[h]	0.88 (0.91)[h]	0.83 (0.89)[h]	0.89 (0.92)[h]

[a] In dichloromethane, at 22 °C, unless noted otherwise. [b] From ref 41, unless noted otherwise. [c] From ref 22a. [d] From Fukuzumi, S.; Kochi, J. *J. Org. Chem.* **1981**, *46*, 4116. [e] From ref 12b. [f] Unpublished results. [g] From ref 4f. [h] Data in parentheses in acetonitrile.

The striking fit of all the data to a single linear correlation with $a \approx 1.0$ in eq 3 (with correlation coefficient > 0.99) provided compelling evidence that the precursor complex between an electron acceptor and its anion radical in fact derived from the charge-transfer interaction as originally defined by Mulliken.[13] In accord with this conclusion, the precursor complex will hereafter be interchangeably referred to as the anion-radical π-mer, in which the NIR absorption corresponds to the *homonuclear* charge-transfer band.[24] Thus, the anion-radical π-mer as a negatively charged homomolecular dimer is to be also considered together with the other (uncharged) electron donor/acceptor complexes, which then represent their heteromolecular analogues.

IV. Intermolecular Binding in Precursor Complexes (Theoretical Basis). Electron donor−acceptor complexes in the general context of Mulliken theory are generated by the linear combination of the principal van der Waals ($\psi_{D,A}$) and dative ($\psi_{D^+A^-}$) states. Such an intermolecular charge-transfer interaction is conveniently described via the valence-bond approach, so that the ground-state and excited-state wave functions can be expressed as[25]

$$\Psi_{GS} = a\psi_{D,A} + b\psi_{D^+A^-} \quad (5)$$

$$\Psi_{ES} = b\psi_{D,A} - a\psi_{D^+A^-} \quad (6)$$

The energies of the ground and excited states obtained from

(21) For example, in studies of electron-transfer self-exchange of lithium, sodium, and potassium salts of the anion radicals of TCNQ and TCNE in acetonitrile, the same (TCNQ) or very close (TCNE) rate constants were obtained by Komarynsky at al.[8a] Similarly, the electron-transfer self-exchange of TCNE was considered to occur between free ions by Watts et al.[8c] Note, however, that in the less polar dimethoxyethane, the process was considered to be those of loose (solvent-separated) ion pairs.[8c] Similarly, noticeable counterion effects on the kinetic parameters were found for the TCNE anion radical in dimethoxyethane by Ogasawara, M., et al.[8d]

(22) (a) Foster, R. *Organic Charge-Transfer Complexes*; Academic: New York, 1969. (b) Briegleb, G. *Electronen-Donator-Acceptor Komplexe*; Springer: Berlin, 1961. See also the footnotes in Table 2.

(23) The direct relationship of the NIR bands of aromatic cation-radical π-mers to the charge-transfer bands of the same donor with the acceptors in this study was shown by Kochi et al. in ref 12.

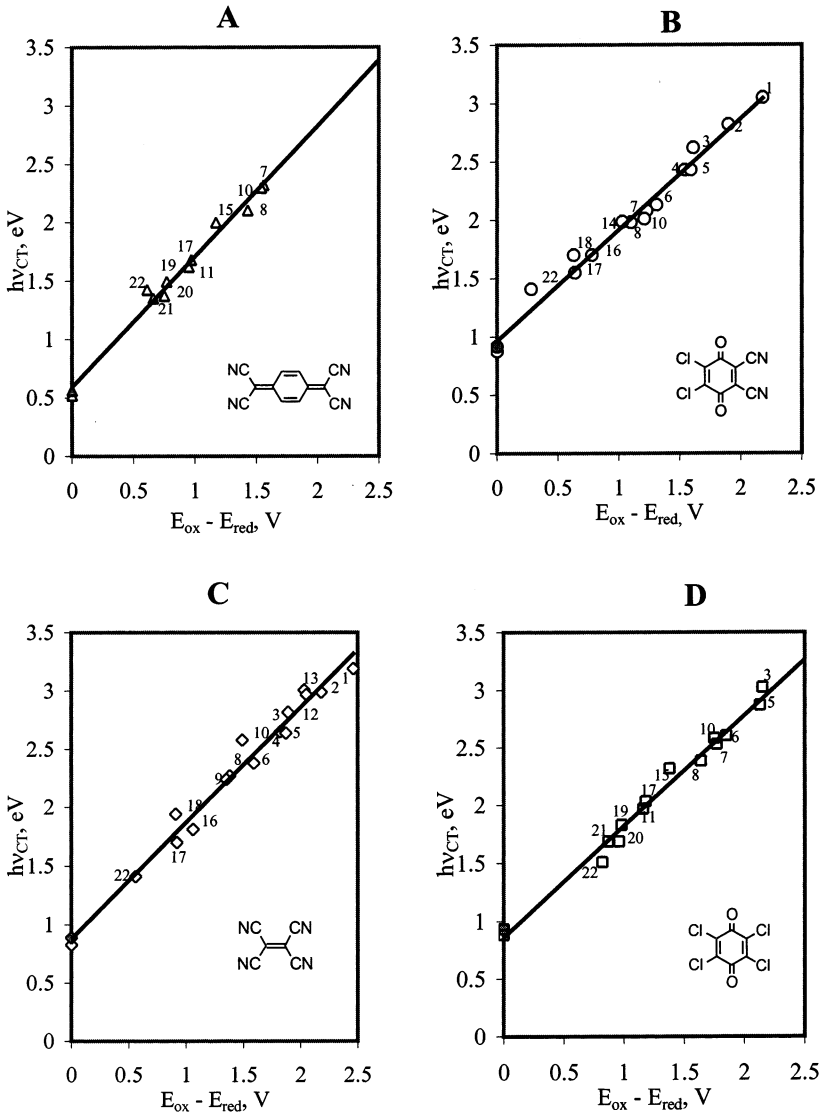

Figure 3. Mulliken correlations (including linear regression lines) for the charge-transfer complexes of TCNQ (A), DDQ (B), TCNE (C), and CA (D) with different organic donors in dichloromethane solutions. Numbers near points identify the donors in Table 2. Corresponding π-mers [$(TCNQ_2)^{-\bullet}$ (A), $(DDQ_2)^{-\bullet}$ (B), $(TCNE_2)^{-\bullet}$ (C), and $(CA_2)^{-\bullet}$ (D)] presented by points on the *y*-axes. [Note that unfilled points correspond to dichloromethane solution, and filled points to the acetonitrile solution].

the solution of the secular equation by the variational method (constraining the mixing coefficients to the normalized $a^2 + b^2 = 1$ and neglecting the overlap, i.e., $\int \psi_{D^+A^-} \psi_{D,A} = 0$) can be expressed as[25]

$$E_{GS} = (\epsilon_{D,A} + \epsilon_{D^+A^-})/2 - (\Delta^2 + 4H_{DA}{}^2)^{1/2}/2 \qquad (7)$$

$$E_{ES} = (\epsilon_{D,A} + \epsilon_{D^+A^-})/2 + (\Delta^2 + 4H_{DA}{}^2)^{1/2}/2 \qquad (8)$$

where the Coulomb integrals $\int \psi_{D,A} H \psi_{D,A}$ and $\int \psi_{D^+A^-} H \psi_{D^+A^-}$ represent the energies $\epsilon_{D,A}$ and $\epsilon_{D^+A^-}$ of the van der Waals and the dative states, respectively. The energy gap is $\Delta = \epsilon_{D^+A^-} - \epsilon_{D,A}$, and the electronic coupling matrix element is given by the resonance integral $\int \psi_{D,A} H \psi_{D^+A^-} = H_{DA}$. The mixing coefficients that determine the donor/acceptor electron density distribution at the energy minimum are related to the electronic coupling element as $c_a c_b = H_{DA}/(E_{ES} - E_{GS})$, and the energy of the optical transition from eqs 7 and 8 is

$$\nu_{CT} = E_{ES} - E_{GS} = (\Delta^2 + 4H_{DA}{}^2)^{1/2} \qquad (9)$$

Traditional studies of charge-transfer complexes deal mainly with static donor/acceptor systems in which oxidation potential of the donor is substantially higher than the reduction potential of the acceptor.[22] Therefore, (complete) electron transfer is energetically unfavorable, and the donor/acceptor interaction results in the formation of more or less thermodynamically stable complexes. Transient precursor complexes [**D**,**A**] formed via the intermolecular donor/acceptor interaction in the course of an electron-transfer reaction in eq 1 bear the same earmarks as classical charge-transfer complexes. Hush and Sutin showed how the combination of the Mulliken (charge-transfer) formalism

(24) Since we consider anion-radical π-mers as localized systems (vide infra), the NIR bands in the $(\mathbf{A_2})^{-\bullet}$ complex are referred to as charge-transfer transitions. However, the analogous electronic absorptions in cation-radical π-mers have been referred to as charge-resonance bands.[11,12]

(25) (a) Brunschwig, B. S.; Sutin, N. Reflections on the two-state electron-transfer model. In *Electron Transfer in Chemistry*; Balzani, V., Ed.; Wiley: New York, 2001; Vol. 2, p 583. (b) Brunschwig, B. S.; Sutin, N. *Coord. Chem. Rev.* **1999**, *187*, 233. (c) Sutin, N. *Adv. Chem. Phys.* **1999**, *106*, 7. (d) Creutz, C.; Newton, M. D.; Sutin, N. *J. Photochem. Photobiol. A*: *Chem.* **1994**, *82*, 47.

Table 3. Mulliken−Hush Analysis of the Electronic Coupling Element in Anion Radical (Precursor) Complexes with the Parent Acceptors[a]

precursor complex	ν_{CT} (10^3 cm^{-1})	$\Delta\nu_{CT}$ (10^3 cm^{-1})	ϵ (10^3 M^{-1} cm^{-1})	H_{DA} (10^3 cm^{-1})
$(TCNQ)_2^{-\bullet}$	4.6	2.2	3.2	1.15
$(DDQ)_2^{-\bullet}$	7.3	2.7	1.6	1.10
$(TCNE)_2^{-\bullet}$	7.2	2.8	0.8	0.79
$(CA)_2^{-\bullet}$	7.4	2.7	1.3	1.00

[a] In acetonitrile at 22 °C.

with the Marcus (quadratic) representation of initial and final diabatic states of the redox process allows the potential-energy surface for electron transfer to be constructed.[1,25] Most importantly, such a marriage of the static CT and the dynamic ET theories explicitly and quantitatively takes into account the precursor complex.[1,25] Furthermore, such a combination focuses on the direct relationship between the optical and thermal electron transfer in the donor/acceptor dyads, and this methodology allows the electron-transfer dynamics to be evaluated from the spectral characteristics of the precursor complex.[25,26] According to this Marcus−Hush−Sutin (MHS) formalism, the Marcus reorganization energy λ is equal to the energy of the charge-transfer transition $h\nu_{CT}$ in the absence of a driving-force contribution to electron transfer. The electronic coupling element H_{DA} in the precursor complex is evaluated experimentally from the spectral data as[27]

$$H_{DA} = 0.0206(\nu_{CT}\Delta\nu_{1/2}\epsilon_{CT})^{1/2}/r_{DA} \qquad (10)$$

where ν_{CT} and $\Delta\nu_{1/2}$ are the spectral maximum and full-width at half-maximum (cm^{-1}), respectively, of the charge-transfer absorption band, ϵ_{CT} is the extinction coefficient (M^{-1}cm^{-1}) of the precursor complex, and r_{DA} is the separation (Å) between the redox centers. Although the development of the MHS approach was originally based on mixed-valence complexes in which the redox centers are fixed by a connecting bridge,[4,26] this limitation largely resulted from the singular absence of intermolecular systems heretofore in which the precursor complexes could be experimentally detected and thoroughly characterized.

Discussion

The structural and spectral characterization of the anion-radical π-mer as the precursor complex in self-exchange electron transfer as examined in Tables 1−3 now allows us to implement the MHS methodology in intermolecular ET processes. Since such an analysis requires the structural characteristics of the complex (especially the separation parameter r_{DA} in eq 10), let us first turn to the structures of anion-radical π-mers.

I. Structure of the Precursor Complex in Self-Exchange. The molecular associations of the electron acceptors **A** in Chart 1 with their anion radicals $\mathbf{A}^{-\bullet}$ in solution (Table 1) are considered to be weak, typically with values of $K_{PC} < 10$ M^{-1}. The structural nature of the intermolecular binding of **A** and $\mathbf{A}^{-\bullet}$ to form the negatively charged precursor complex ($\mathbf{A_2}^{-\bullet}$) is indicated by the X-ray crystal structure of the tetracyano-

Chart 3

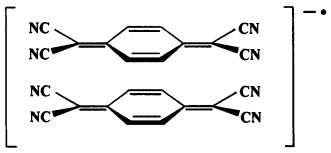

quinodimethane complex schematically illustrated in Chart 3,[28] in which the TCNQ and $TCNQ^{-\bullet}$ moieties lie cofacially atop one another and somewhat shifted with an interplanar separation of about $r_{DA} = 3.2$ Å.[17] Both moieties in the dimeric salts of $(TCNQ)_2^{-\bullet}$ are structurally intermediate between that of the parent TCNQ and that of the slightly enlarged anion radical,[17] as shown in Chart 2. The face-to-face arrangement of the nearly planar moieties in the corresponding mixed complex (anion radical/neutral acceptor) with an interplanar distance about 2.9 Å is also obtained in the DDQ systems. Although the association in Figure 1 includes a pair of anion radicals with one neutral acceptor, the first step of such a [2:1] complex formation must proceed via the [1:1] complex. As such, half of the [2:1] complex is a reasonable approximation for r_{DA}= 3.3 Å in the anion-radical π-mer. Additional insight into the structure of such π-mers can be obtained from the analysis of the structural features of other charge-transfer complexes of the corresponding acceptors. Thus, charge-transfer complexes formed by the π-acceptors under study with different (uncharged) planar donors are generally characterized by face-to-face arrangements with slightly higher interplanar donor/acceptor distances of about 3.5 Å.[29] Such an arrangement is similar to the experimentally determined structure of the anion-radical π-mer of $TCNQ^{-\bullet}$, and there is a reasonable basis to conclude that the structures of the precursor complex with the quinone systems $(DDQ)_2^{-\bullet}$ and $(CA)_2^{-\bullet}$, as well as that of the tetracyanoethylene system $(TCNE)_2^{-\bullet}$ are close to that found for $(TCNQ)_2^{-\bullet}$. Accordingly, we will take 3.3 Å to be a reasonable average for the interplanar separations in the anion-radical π-mers generally.[28]

II. Electron Exchange within the Precursor Complex. Electron (self) exchange rates between various electron acceptors and their anion radicals have been measured by the concentration-dependent line-broadening of the ESR spectra.[7,8] However, such measurements in solution are incapable of distinguishing diffusional electron transfers from those taking place within the precursor complex. To address the latter, we note that the electronic interaction of $\mathbf{A}/\mathbf{A}^{-\bullet}$ moieties in the intermolecular precursor complex is related to that previously encountered in the *intramolecular* mixed-valence compounds in which the redox centers are deliberately tied together by a molecular bridge.[4,26] In such systems, the electronic interaction of **A** with $\mathbf{A}^{-\bullet}$ is evaluated by the magnitude of the electronic coupling element H_{DA} (Table 3), and the rate of electron transfer between them in governed by the Marcus reorganization energy λ.[4]

Figure 4 shows the plots of the free-energy change along the reaction coordinate for the self-exchange electron transfer

(26) (a) Creutz, C. *Prog. Inorg. Chem*. **1983**, *30*, 1. (b) Omberg, K. M.; Chen, P.; Meyer, T. J. *Adv. Chem. Phys.* **1999**, *106* (part 1), 553. (c) Demadis, K. D.; Hartshorn, C. M.; Meyer, T. J. *Chem. Rev.* **2001**, *101*, 2655.

(27) (a) Hush, N. S. *Z. Electrochem*. **1957**, *61*, 734. (b) Hush, N. S. *Trans. Faraday Soc*. **1961**, *57*, 557. (c) Hush, N. S. *Prog. Inorg. Chem*. **1967**, *8*, 391. (d) Hush, N. S. *Electrochim. Acta* **1968**, *13*, 1005.

(28) (a) Note also the possibility of (planar) slippage as in Figure 1. (b) As a molecular parameter, r_{DA} in eq 10 is difficult to define exactly in intermolecular (optical and thermal) electron transfer, especially owing to variable interplanar distances and the possibility of slippage. In addition, the value of r_{DA} obtained from molecular geometry of complex with substantial coupling undoubtedly requires further correction, and it can be substantially less than the sum of van der Waals radii, as discussed by Newton.[c] (c) Newton, M. D Electron Transfer: Theoretical Models and Computational Implementation. In *Electron Transfer in Chemistry*; Balzani, V., Ed.; Vol. 1, Wiley: New York, 2001; p 3.

(29) (a) Rathore, R.; Lindeman, S.; Kochi, J. *J. Am. Chem. Soc.* **1997**, *119*, 9393.

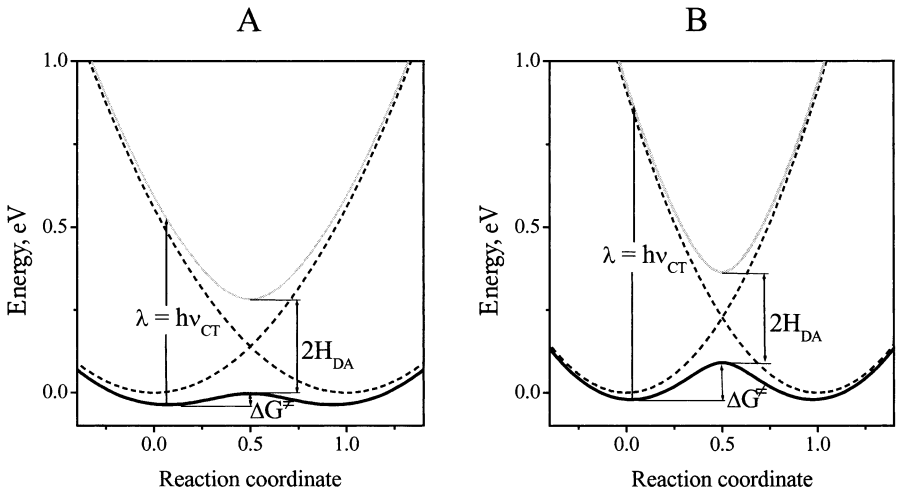

Figure 4. Energy diagrams for electron transfer based on the diabatic reactants (left) and products (right) states (dashed lines) and showing the adiabatic ground state as the precursor complexes for $(TCNQ_2)^{-\bullet}$ (A) and for $(DDQ_2)^{-\bullet}$ (B) in black solid lines and their excited states in gray solid lines.

between **A** and $\mathbf{A}^{-\bullet}$ moieties with $\Delta G^0 = 0$. The dashed parabolic curve on the left (r) represents the reactants diabatic (noninteracting) state between **A** and $\underline{\mathbf{A}}^{-\bullet}$, and that on the right (p) is the products diabatic state between $\mathbf{A}^{-\bullet}$ and $\underline{\mathbf{A}}$ [The underline is simply a label; otherwise **A** and $\underline{\mathbf{A}}$ are identical.] The reorganization energy is given by the vertical (optical) transition with[25] $\lambda = \nu_{CT}$ as listed in Table 3. The values of H_{DA} evaluated from the spectral data in Table 1 according to eq 10 are listed in Table 3.

Within the framework of the Robin-Day classification of mixed-valence compounds,[30] the increasing magnitudes of the electronic coupling reflect the progressive transition from Class I ($H_{DA} = 0$, noninteracting redox centers), to Class II ($0 < H_{DA} < \lambda/2$), and to Class III ($H_{DA} > \lambda/2$, delocalized) systems.[25] Inspection of the results in Table 3 clearly reveals that the precursor complexes relevant to the acceptors in Chart 1 are to be classified as Class II systems since $H_{DA} < \lambda/2$ in all cases. This conclusion is also supported by the consistently lower CT energies in dichloromethane relative to those in acetonitrile. Such shifts are characteristic of Robin-Day Class II systems, connected with the higher (outer-sphere) reorganization energy in the more polar solvent.[8,25]

The evaluations of H_{DA} and λ in Table 3 allow the free-energy profile for electron exchange within the precursor complexes to be constructed within the two-state model.[25] The lower (heavy) lines in Figure 4A,B trace the energy profiles for the prototypical acceptor systems $(DDQ)_2^{-\bullet}$ and $(TCNQ)_2^{-\bullet}$, and the activation free energy for intracomplex electron transfer is presented as $\Delta G^* = 2.6$ and 0.8 kcal mol^{-1}, respectively. In both systems, the transition-state energies for adiabatic electron transfer are substantially less than the value of $\lambda/4$ (determined at the intersection of the diabatic curves). This discrepancy is especially pronounced for $(TCNQ)_2^{-\bullet}$, and the situation with $(TCNE)_2^{-\bullet}$ and $(CA)_2^{-\bullet}$ is similar to that of $(DDQ)_2^{-\bullet}$ (see Figure S3 in the Supporting Information).[31] In other words, as a result of the electronic coupling within the acceptor/anion-radical complex, the intermolecular rates between **A** and $\mathbf{A}^{-\bullet}$ moieties are faster than those predicted simply by an outer-sphere mechanism in which the electronic coupling H_{DA} is small and does not affect the ET barrier evaluated from $\Delta G^* = \lambda/4$.[4-8] We thus conclude that the electronic effects of strong donor/acceptor interactions must be explicitly taken into account in any theoretical description of the self-exchange. To validate the applicability of the electronic parameters obtained via the study of optical transitions to the description of thermal (adiabatic) electron transfer, we now compare the theoretical predictions with those from the available experimental data in the following way.

III. Electron-Transfer Kinetics for Self-Exchange Based on the Precursor Complex. The generalized pathway for electron-transfer self-exchange between an acceptor and its anion radical that includes the precursor complex can be described from Figure 4 as shown in Scheme 1, where K_{PC} is the formation

Scheme 1

$$\underline{\mathbf{A}} + \mathbf{A}^{-\bullet} \overset{K_{PC}}{\rightleftharpoons} [\underline{\mathbf{A}},\mathbf{A}^{-\bullet}] \overset{k_{et}}{\rightleftharpoons} [\underline{\mathbf{A}}^{-\bullet},\mathbf{A}] \rightleftharpoons \underline{\mathbf{A}}^{-\bullet} + \mathbf{A} \qquad (11)$$

constant of the precursor complex (Table 1) and k_{et} is electron exchange rate constant within the precursor complex.[1] The second-order rate constant for intermolecular electron transfer is then given by

$$k_2 = K_{PC}k_{et} \qquad (12)$$

and the intramolecular rate constant can be evaluated from

$$k_{et} = k\nu_n \exp(-\Delta G^*/RT) \qquad (13)$$

where k is the electronic transmission coefficient, ν_n is the nuclear vibration frequency related to electron transfer,[32] and ΔG^* is the free energy of activation for electron transfer.[1] When the electronic coupling is sufficiently strong (as given in Table 3), the activation barriers is[25]

$$\Delta G^* = (\lambda - 2H_{DA})^2/4\lambda \qquad (14)$$

(30) Robin, M. B.; Day, P. *Adv. Inorg. Chem. Radiochem.* **1967**, *10*, 247.
(31) Note that quadratic dependencies of the diabatic states on the reaction (nuclear configuration) coordinates are used in Figure 4 in accordance with the Marcus formulation.[5]
(32) The electronic transmission coefficient represents the probability that electron transfer will occur once the system has reached the intersection region (transition state), and ν_n is the nuclear frequency that takes the system through this region.

Table 4. Comparison of the Experimental (ESR) and Theoretical (Optical) Electron-Transfer Rate Constant for the Acceptor/Anion-Radical Self-Exchange[a]

acceptor	λ[b] (kcal/mol)	H_{DA}[c] (kcal/mol)	ΔG^*[d] (kcal/mol)	k_{et}[e] (10^9 s^{-1})	K_a[f] (M^{-1})	k_2[g] (10^9 M^{-1} s^{-1})	k_{SE}^{theor}[h] (10^9 M^{-1} s^{-1})	k_{SE}^{obs} (10^9 M^{-1} s^{-1})[i,j]
DDQ	21.4	3.2	2.6	12	3	36	12	2.5[i]
TCNQ	13.5	3.4	0.8	240	5	1200	18	3.8[j]
TCNE	21.1	2.3	3.2	4.3	0.5	2.2	1.9	2.2[j]
CA	21.7	2.9	2.9	7.5	4	30	11	

[a] In acetonitrile, at 22 °C, tetrabutylammonium counterion. [b] Reorganization energy, based on data from Table 3 ($\lambda = \nu_{CT}$). [c] Data from Table 3. [d] From eq 14, based on λ and H_{DA} from columns 2 and 3. [e] From eq 13 with ΔG^* from column 3 and $k\nu = 10^{12}$ s^{-1}.[34] [f] From Table 1. [g] From eq 12 based on k_{et} and K_a from columns 5 and 6. [h] From eq 15. [i] Reference 8e. [j] Reference 8h.

owing to adiabatic electron transfer with $k \approx 1$.[33] The calculated values of the bimolecular electron transfer obtained from the measured value of K_{PC} in Table 1, together with the reorganization energy, the electron coupling element (obtained from the theoretical evaluation of the precursor complex in Table 3), and $\nu_n = 10^{12}$ s^{-1} [34] lead to the second-order rate constants that lie in the range 10^9-10^{10} M^{-1} s^{-1} (Table 4). For such fast reactions, the effects of diffusion (k_{diff}) must be explicitly taken into account.[7,8] Thus, for comparison with the experimental values of the self-exchange rate constant (k_{SE}), the theoretical rate constant is corrected as

$$1/k_{SE}^{theor} = 1/k_2 + 1/k_{diff} \qquad (15)$$

where k_2 is the second-order rate constant without the diffusional correction, and k_{diff} is taken as 1.9×10^{10} M^{-1} s^{-1} in acetonitrile at 22 C.[8f] The theoretically predicted rate constants (k_{SE}^{theor}) evaluated in this manner are compared with the experimental values (k^{obs}) in the last two columns of Table 4. We consider the agreement between these to be satisfactory, especially if we take into account the uncertainty in the evaluation of the preexponential factor in eq 13.[34] Although a more rigorous comparison of the experimental and theoretical rate constants is desirable (particularly in the preexponential factor), the analysis of the extant data allows several important conclusions to drawn.

A. Validation of the Marcus−Hush−Sutin Methodology. Although there were several previous attempts at the estimation of electron-transfer rate constants based on H_{DA} and λ derived from optical data,[3,4] only the results of this study allow the direct comparison of the theoretically predicted and the experimentally determined rate constant for electron-transfer self-exchange in *intermolecular* processes such as those based on ESR line-broadening measurements.[35a] The agreement obtained in Table 4 indicates that the MHS methodology provides reasonable evaluations of the electronic coupling interaction (H_{DA}) and the reorganization energy (λ) for the intermolecular electron-transfer process between an electron acceptor and its anion radical (despite the possibility of some overlap in anion-radical complexes[35b]). Indeed, the earlier (substantial) underestimation[6−8] of the predicted rate constants in anion-radical self-exchange processes can be directly attributed to the neglect of the strong electronic interaction in the precursor complex in the theoretical calculation of the activation barrier.

B. Evaluation of the Reorganization Energy for Self-Exchange. The optical data in Table 3 allow us to verify the previous estimates of the reorganization energy in such systems. According to Marcus theory, the overall reorganization energy λ is expressed as the sum of the inner-sphere reorganization energy λ_i and the outer-sphere term λ_o (which represent the energy of solvent reorganization). Inner-sphere reorganization energies can be evaluated from the bond length/angle differences between the oxidized and reduced species that participate in the redox process (see Chart 2), together with the corresponding force constants.[36] Outer-sphere reorganization is usually calculated from the effective radii of the reactants considered as either spheres or ellipsoids, the reaction distance, and the Born model of the solvent as a continuous dielectric medium.[36] On the other hand, the reorganization energy λ is usually evaluated experimentally from the kinetics of the self-exchange processes, based on the simple relationship

$$k_2 = Z \exp(-\Delta G^*/RT) \qquad (16)$$

with $\Delta G^* = \lambda/4$ and collision frequency $Z = 10^{11}$ M^{-1} s^{-1}.[7,8]

(33) When the electronic interaction between the reactants is weak, $k_{el} \ll 1$, and the electron transfer occurs in the *nonadiabatic* regime. In such a case $\Delta G^* = \lambda/4$ (where $\lambda = \lambda_{in} + \lambda_o$) and $k_{el}\nu_n = \nu_{el} = (2H_{DA}^2/h)(\pi^3/\lambda RT)$. Thus, when the electronic coupling is weak (nonadiabatic limit), H_{DA} explicitly determines the preexponential factor (or probability of electron transfer in the transition state). When the electronic interaction is strong (strongly adiabatic limit), H_{DA} affects the exponential factor (i.e., transition-state energy). Therefore, eq 16, which is frequently used for the estimation of the intermolecular electron-transfer rate constant,[6−8] is valid only in a very limited range of H_{DA} values (usually from about 30−50 to 150−200 cm^{-1}).

(34) Since the electron-transfer self-exchanges of anion radicals involve numerous molecular (∼500−3000 cm^{-1}) and solvent (∼10−100 cm^{-1}) vibrational modes, the preexponential factor $\nu_n = (\sum \nu_i^2\lambda_i/\sum\lambda_i)^{1/2}$ [as described by Sutin[1]] is difficult to rigorously calculate from the available data. Thus for this study, we have simply taken ν_n to be uniformly 10^{12} s^{-1}, a value similar to those previously used for the description of electron transfers in coordination compounds (approximated by few modes) or taken a priori as kT/h.[1,26] According to Sutin, such a choice derives from the effective frequency that is dominated by solvent modes, especially when the solvent barrier is relatively large (although the frequency of the intramolecular vibrations is substantially higher). Most importantly, this choice leads to calculated rate constants that agree with the experimental kinetics (Table 4), and a substantial increase in the preexponential factor will shift the rate constants to the (unrealistic) diffusion-controlled limit.

(35) (a) For a similar application of the MHS (two-state) model to intermolecular electron transfer of arene donors with NO^+ via of the [1:1] precursor complex (Class III), see: Rosokha, S. V.; Kochi, J. K. *New J. Chem.* **2002**, *26*, 851. (b) Since the MHS (two-state) model requires the diabatic states to be orthogonal,[25d] the small orbital overlap that may exist in anion-radical complexes may necessitate some correction of the parameters obtained via eqs 8−14. However, Creutz et al.[25d] successfully applied the MHS model to ruthenium complexes (with a similar overlap problem), and we depend on the same approach. In particular, we judge the validity of the two-state model by recognizing the reasonable correspondence between the experimental and theoretically predicted rate constants presented in Table 4. Clearly, a more quantitative analysis will ultimately be needed, the impetus for this being hopefully provided from studies such as that described herein.

(36) (a) If donor/acceptor separation in electron transfer is larger than the sum of their radii, the relationship is $\lambda_0 = (e_oN_A/4\pi\epsilon_0)g(r,d')\gamma$, where $\gamma = 1/\epsilon_o - 1/\epsilon_s$ (ϵ_o and ϵ_s are the optical and static dielectric constants), and $g(r,d')$ is a function of the effective molecular radius as described by Grampp et al. in ref 8f. (b) However, note that for the cofacial arrangement of planar reactants in the precursor complex the previous estimates based on a point-dipole-in-a-sphere model (with the sphere corresponding to the precursor complex having the overall radius of the reactant pair) lead to values of λ_o that can be off by a factor of 2 (or more) relative to one that considers the reactants as touching spheres or ellipsoids.[8a] (c) For the quantum-mechanical calculation of the inner-sphere reorganization energy, see refs 7j−o.

Table 5. Comparison of the Experimental and Theoretical Reorganization Energies for $A^{-\bullet}/A$ Self-Exchange[a]

acceptor	λ_i^{theor} (kcal/mol)	λ_o^{theor} (kcal/mol)	$\lambda^{theor\ e}$ (kcal/mol)	$\lambda_{SE}{}^f$ (kcal/mol)	λ^g (kcal/mol)
DDQ	10.0[b]	19.5[b]	29.5	8.4	21.4
TCNQ	6.4[c]	22.4[d]	28.8	7.2	13.5
TCNE	3.3[c]	26.0[d]	29.2	8.8	21.1

[a] In acetonitrile, at 22 °C. [b] Reference 8e. [c] Reference 8f. [d] Reference 6d. [e] Obtained as $\lambda_i^{theor} + \lambda_o^{theor}$ from columns 2 and 3. [f] Experimental reorganization energy estimated as $4\Delta G^*$ from the self-exchange kinetics [ΔG^* is calculated via eq 16 using $Z = 10^{11}$ M^{-1} s^{-1} (collision frequency) and $k_2 = (1/k_{SE}^{obs} - 1/k_{diff})^{-1}$, where k_{SE}^{obs} is taken from the last column in Table 4 and $k_{diff} = 1.9 \times 10^{10}$ M^{-1} s^{-1}]. [g] Experimental reorganization energy evaluated from the charge-transfer (NIR) absorption band of the corresponding complex.

In the case of outer-sphere redox processes of coordination compounds, the theoretically estimated reorganization energy generally allows satisfactory predictions of the rate constants for the self-exchange processes.[1] In other words, the theoretically predicted reorganization energy in outer-sphere electron transfer is close to that experimentally determined from the kinetic data based on $\lambda = 4\Delta G^*$. However, in the case of self-exchange processes for electron transfer of organic molecules, the theoretically predicted reorganization energy is in many cases substantially larger than that evaluated from the kinetic data. [For example, see the analysis presented by Eberson in ref 5 for large numbers of organic systems.] In particular, for the π-acceptors in Chart 1, the theoretical estimates of λ^{theor} (column 4 in Table 5) are roughly 400% larger than λ_{SE} evaluated simply as $4\Delta G^*$ obtained from the kinetic data, and the results obtained in this study clarify such discrepancies of the reorganization energies in the following way. First, the strong electronic interaction between the donor/acceptor moieties within the precursor complex leads to substantial lowering (40−75%) of the activation barrier for electron transfer relative to that simply based on $\lambda/4$. Therefore, the relationship $\Delta G^* = \lambda/4$, which is valid for weakly interacting systems, is not generally a reliable method for the evaluation of the reorganization energy, particularly of π-systems. [This is seen from a comparison of data in columns 5 and 6 in Table 5 with λ_{SE} estimated from self-exchange kinetics which are substantially lower than λ obtained from optical data.] Second, the reorganization energies in Table 3 that are experimentally derived from the optical data are substantially lower than the theoretical estimates of λ^{theor} cited in the literature (compare columns 4 and 6 in Table 5).[6−8] This discrepancy is at least partially ascribable to the neglect of the precursor complex in which the planar donor/acceptor dyads lie intimately (i.e., face-to-face) and largely preclude any intervening solvent from the activated complex.[8a] Such transition-state structures must clearly be recognized in redox processes of organic π-donors, especially those of the aromatic analogues with nonspherical shapes. Thus, a theoretical calculation can overestimate the reorganization energy due to enhancement of the outer-sphere component, and the calculations of the reorganization energy based on self-exchange kinetics can substantially underestimate its real value owing to the effective lowering of the barrier due to the strong electronic interaction, such that $\Delta G^* < \lambda/4$. [It is interesting to note that since the electronic coupling in the precursor complexes in the cross-exchange is expected to be less effective (due to symmetry reasons), the values of reorganization energy estimated from cross-exchange can actually be higher than those estimated from self-exchange kinetics, as reported earlier by Nelsen et al.[2]]

C. Mechanism for Self-Exchange and the Evaluation of H_{DA}. The kinetics formulation in Scheme 1 can be used to verify estimates of the electronic coupling element, particularly for the organic redox processes under discussion. Thus the values of H_{DA} established for the self-exchange electron transfers of $TCNQ^{-\bullet}$ and $DDQ^{-\bullet}$ in Table 3 agree with the theoretical molecular orbital calculations, while the experimental value for $TCNE^{-\bullet}$ is substantially larger than the predicted one.[8] Although other theoretical data are not yet available, the values of H_{DA} in Table 3 generally correspond to the estimates based on the indirect analysis of anion-radical (redox) kinetics by Eberson and Shaik[37] from a different perspective. Most importantly, the sizable values of H_{DA} relative to the reorganization barrier cannot be neglected in any prediction of the activation barrier for electron transfer, and significant rate increases do result from the decrease of the TCNQ barrier by roughly 75%, of the DDQ and CA barrier by 50%, and of the TCNE barrier by 40% according to the significant presence of the precursor complex as formulated in Scheme 1.

IV. Comments on the Role of the Precursor Complex in Outer-Sphere and Inner-Sphere (Electron-Transfer) Mechanisms. The precursor complex in outer-sphere electron transfer between a donor and acceptor according to Taube[38] involves no bond breaking or bond forming (ligand exchange) prior to the activated complex. Likewise in Marcus theory,[1,5] the outer-sphere precursor complex is limited to only weak (unperturbed) donor/acceptor interactions, in which the probability of electron transfer is close to unity (adiabatic) or substantially less than unity (nonadiabatic). As a result, most quantitative studies of basic electron transfer (experiment and theory) have focused primarily on outer-sphere processes.[1,3,6,39] However, when the redox centers are intimately shared (as in ligand exchange), the inner-sphere process must involve stronger intermolecular electronic interactions and substantial increases in electron-transfer rates. Heretofore, the effects of the strong donor/acceptor coupling in the inner-sphere precursor complexes have been considered only qualitatively, the sole exception being the intramolecular mixed-valence complexes in which the donor/acceptor centers are directly bridged, as in the original Creutz−Taube ion and other organic analogues.[4,27,40] Since the present study clearly demonstrates how the electronic coupling in the precursor complex can dramatically affect the dynamics of intermolecular electron transfer, let us briefly consider how our conclusions impinge on various redox systems more generally.

The quantitative analyses of synthetically significant organic processes involving a critical electron-transfer step reveal strong donor/acceptor interactions indicative of the inner-sphere pathway.[41] We believe the inner-sphere precursor complex is important whenever the reactant structure allows substantial overlap of the donor/acceptor orbitals. Thus, organic systems such as planar aromatic donors and acceptors (unencumbered

(37) Eberson, L.; Shaik, S. S. *J. Am. Chem. Soc.* **1990**, *112*, 4484.
(38) Taube, H. *Electron-Transfer Reactions of Complex Ions in Solution;* Academic Press: New York, 1970.
(39) Moreover, as recently noted by Bixon and Jortner, "... the majority of thermal outer-sphere ET in solution and photoinduced ET via bridges in organic and inorganic supermolecules proceed via non-adiabatic ET...". See: Bixon, M.; Jortner, J. *Adv. Chem. Phys.* **1999**, *106* (part 1), 35.
(40) Haim, A. *Prog. Inorg. Chem.* **1983**, *30*, 273.
(41) Rathore, R.; Kochi, J. K. *Adv. Phys. Org. Chem.* **2000**, *35*, 193.

by bulky substituents), as well as sterically accessible inorganic complexes such as the linear Ag(I) and Hg(II), trigonal Al(III), and square-planar nickel(II) and copper(II), etc., are prone to interact with relatively small reagents such as Br_2, NO^+, Cl_2^-, $S_2O_8^{2-}$, and H_2O_2 to form transient inner-sphere complexes.

Despite their seminal importance in the development of electron-transfer theory, the weakly interacting donor/acceptor dyads in outer-sphere electron transfer actually represent a minority and are largely limited to coordinatively saturated (octahedral) complexes and involve rather long-range electron transfer. In this regard, let us reconsider Taube's traditional classification (centered as it is on only inorganic coordination compounds) in a broader quantitative context for the following reasons: (1) A viable electron-transfer classification should include the wide spectrum of organic, inorganic, and biochemical donor/acceptor dyads, *independent* of the presence of ligands; (2) the span of donor/acceptor interactions should be considered incrementally from nonadiabatic electron transfer of weakly bound dyads at one extreme to those involving chemical bonds at the other extreme; (3) strongly interacting donor/acceptor dyads merit more careful and quantitative consideration since they will include chemically important redox systems for electrical conductors, magnets, sensors, etc., of potential relevance to material science.

Mechanistic Proposal. Owing to the importance of the electronic coupling element H_{DA} to the redox characteristics of the precursor complex, we follow Sutin's development of the two-state model,[1,25] the Robin-Day classification,[30] together with Nelsen's suggestion,[42] and employ the normalized ratio H_{DA}/λ as the single parameter[43] to classify electron-transfer mechanisms, especially as a basis for further study and comment.

Outer-Sphere Mechanism with $H_{DA}/\lambda < 0.025$. In this limited region, the effects of H_{DA} on the activation barrier will be less than 10% (relative to the those calculated as $\lambda/4$). Thus, for redox systems with reorganization energies in the range $\lambda = 25 \pm 15$ kcal/mol, the rate constant will be within an order of magnitude of that without the correction. Since such an uncertainty is insufficient for any mechanistic distinction, this redox process is defined as *outer-sphere*. The outer-sphere precursor complex is likely to be experimentally detected only with additional ion-pairing effects and/or at extremely high concentrations.[3]

Inner-Sphere Mechanism with $H_{DA}/\lambda > 0.025$. For these redox systems, the energy barriers and electron-transfer rates will be substantially affected by the electronic coupling (binding) within the precursor complex, and we correspondingly define such processes as *inner-sphere*. We note that Sutin[26] considers redox systems with $H_{DA} > 200$ cm^{-1} to be strongly adiabatic (Class II), and this coupled with $\lambda \approx 25$ kcal mol^{-1} corresponds to $H_{DA}/\lambda = 0.025$. Accordingly, this proposed definition of inner-sphere electron transfer corresponds to a strongly adiabatic process.

In essence, such a global definition of outer-sphere and inner-sphere electron-transfer mechanisms encompasses the Taube classification, but it is not dependent on structural types. Thus, the new definition allows a variety of donor/acceptor dyads to be included (in addition to coordination compounds), and it thus readily accommodates hybrid redox systems involving organic and inorganic donor/acceptor dyads of particular importance to organometallic and biochemical oxidation−reductions. We envisage a wide (structural) array of redox systems to be included in the inner-sphere pathway. Therefore, to provide an *operational* basis for further studies of inner-sphere electron transfer, we distinguish three subclasses.

(i) Inner-Sphere Systems with $0.025 < H_{DA}/\lambda < 0.1$. The effects of increasing H_{DA} in this range can lead to the lowering of the activation barrier by 10−40% with concomitant increase in the rate constant predictions by 1−2 orders of magnitude. As a result, the precursor complex must be considered explicitly despite the experimental difficulties that may be encountered in the detection/characterization of such weakly interacting associations.[44]

(ii) Inner-Sphere Systems with $0.1 < H_{DA}/\lambda < 0.5$. In this intermediate region, the effects of H_{DA} on the energy barrier can be dramatic, with decreases in the activation barrier of as much as 40%−99% and discrepancies in the rate predictions of more than 3 orders of magnitude. [The self-exchange in the acceptor/anion-radical dyads studied here fall into this category.] Although the association constants are not high, by careful (spectral) analysis it should be possible to experimentally detect and characterize the precursor complex.

(iii) Inner-Sphere Systems with $H_{DA}/\lambda > 0.5$. This extreme region corresponds to Class III in the Robin-Day classification. As such, electron donors form stable complexes with acceptors, which can be characterized spectroscopically and isolated as single crystals for X-ray crystallographic analysis. [Examples of such systems are octamethylbiphenylene cation-radical π-mers with $K_a = 350$ M^{-1} and intermolecular complexes of arenes with nitrosonium (NO^+) which have association constants of up to 10^6 M^{-1}.[12,35a]] The electron is extensively delocalized within such precursor complexes. As such, there is essentially no barrier for electron transfer from the donor to the acceptor, and the electronic interaction within such precursor complexes can be basically considered as strongly bonding.

Summary and Conclusion

The precursor (or encounter) complex, despite its integral role in intermolecular electron-transfer processes, has been largely neglected (or completely overlooked) as a metastable intermediate owing to the paucity of structural data heretofore. To quantitatively establish how the precursor complex is critical to electron-transfer dynamics, we thus focused on the self-exchange kinetics of a series of π-acceptors **A** with their reduced anion radicals $\mathbf{A}^{-\bullet}$ in which the precursor complex is the intermolecular π-mer $\mathbf{A}_2^{-\bullet}$ and can be subjected to thorough structural characterization. Since this basic (redox) system occurs in the absence of a driving-force contribution, the electron-transfer dynamics can be quantitatively evaluated with the aid of only the Marcus reorganization energy (λ) and the intermolecular electronic coupling element (H_{DA}) based on the two-

(42) Nelsen, S. In *Electron Transfer in Chemistry*; Balzani, V., Ed.; Wiley-VCH: New York, 2001; Vol. 1, p 342.

(43) The use of this normalized ratio is based on the fact that H_{DA} and λ determine the barrier for electron transfer (eq 14), the stabilization of precursor complex (as H_{DA}^2/λ), and the charge transferred from the donor to acceptor.[25,35a]

(44) (a) Since the energy gain due to electronic coupling is proportional to H_{DA}^2/λ, the association constant here is expected to be less than 1 M^{-1}, as observed in systems with higher values of H_{DA}/λ. (b) When the optical (charge-transfer) transition is experimentally unobservable, alternative theoretical (quantum mechanical) treatments are favored for the evaluation of H_{DA}.

state Hush−Sutin treatment. Most importantly, we underscore the caveat that the "true" reorganization energy obtained from the optical (charge-transfer) transition inherent to these precursor complexes is *substantially* higher than that obtained from the self-exchange data by the indiscriminate application of Marcus (outer-sphere) theory.

Experimental Section

Materials. Acetonitrile, dichloromethane, acetone, and hexane (Merck) were purified according to standard laboratory procedures[45] and were stored in Schlenk flasks under an argon atmosphere. Neutral acceptors TCNQ, DDQ, TCNE, and CA (Aldrich) were purified by repeated recrystallization and/or sublimation in vacuo. Sodium iodide, lithium iodide, tetrabutylammonium iodide, and tetraethylammonium iodide (Acros) were used as received. Anion-radical salts were prepared by the interaction of the neutral acceptors with 1.5−3 molar excess of the corresponding alkali-metal or alkylammonium iodide. $Bu_4N^+TCNQ^{+\bullet}$ and $Bu_4N^+CA^{+\bullet}$ were isolated after ion-exchange with the corresponding alkali-metal salts.[14,46] Thus, $Li^+TCNQ^{-\bullet}$ was prepared by the addition of a hot solution of 4 g (0.03 mol) of LiI in 10 mL of acetonitrile to a boiling solution of 2.04 g (0.01 mol) of TCNQ in 200 mL of acetonitrile. After cooling and standing for 4 h at room temperature, the solid was collected and successively washed with acetonitrile and ether. Sodium salts of $TCNQ^{-\bullet}$ were prepared in a similar way. To prepare the tetrabutylammonium salt of $TCNQ^{-\bullet}$, the corresponding lithium salt (570 mg) was dissolved in water, and 1.01 g of tetrabutylammonium iodide was added. The blue precipitate was filtered, washed, and air-dried. To prepare $Na^+DDQ^{-\bullet}$, 219 mg (0.96 mmol) of DDQ in 10 mL of acetonitrile was added to 144 mg of NaI in 10 mL of acetonitrile. The volume of the solution was reduced to 8 mL, and the mixture was stored at −30 °C for 3 days. The precipitate was filtered and washed with small amounts of cold acetonitrile. The tetrabutylammonium salt of $DDQ^{-\bullet}$ was prepared similarly. To prepare the sodium salt of $TCNE^{-\bullet}$, 1.1 g of NaI (7.4 mmol) was added to 315 mg (2.5 mmol) of TCNE in 5 mL of acetonitrile. The precipitate formed in the course of 30 min stirring was filtered, washed with dichloromethane, and dried in vaccuo. The tetrabutylammonium salt of TCNE anion radical was prepared similarly. However, a 1.5 mol excess of iodide was used and the solution kept in the refrigerator for 3 days to obtain yellow crystals of $Bu_4N^+TCNE^{-\bullet}$. TCNE anion-radical salts were alternatively prepared by the interaction of the parent acceptor with Na^+CN^- and $Bu_4N^+CN^-$,[46b] but the results did not depend on the reducing agent. The sodium salt of chloranil anion radical was prepared by the slow addition of 780 mg (3.2 mmol) of CA to a solution of 1.44 g (9.6 mmol) of NaI in 100 mL of acetone stirred in a cold bath at 0 °C. Stirring was continued for 2 h, and the precipitate was filtered and washed with small amounts of cold acetone and dichloromethane. The potassium salt of chloranil anion radical was prepared similarly. To prepare the tetrabutylammonium salt of $CA^{-\bullet}$, tetrabutylammonium chloride (233 mg) was added at 0 °C to a solution of $K^+CA^{-\bullet}$ (239 mg) in acetone. The precipitate was filtered, and the filtrate was concentrated in vaccuo to dryness. The residue was recrystalized from a CH_2Cl_2/pentane mixture. The purity of all compounds was checked spectrophotometrically (using the spectral characteristics of anion radicals in Table 1) and by titration with ammonium cerium(IV) nitrate (Acros).

X-ray Crystallography. The intensity data for all the compounds were collected with a Siemens SMART diffractometer equipped with a 1K CCD detector using Mo Kα radiation ($\lambda = 0.71073$ Å) at −150 °C. The structures were solved by direct methods[47] and refined by full matrix least-squares procedure with IBM Pentium and SGI O_2 computers. [Note that the X-ray structure details of compounds mentioned here are on deposit and can be obtained from Cambridge Crystallographic Data Center, U.K.] $(Et_4N^+)_2(DDQ_3)^{2-}$: A 100 mL flask equipped with a Schlenk adapter was charged with 17 mg (about 0.05 mmol) of $(Et)_4N^+DDQ^{-\bullet}$ and 20 mg (about 9 mmol) of DDQ, and 10 mL of dichloromethane was added under argon atmosphere. After dissolution, the solution was covered with hexane and put into a cold (−65 °C) bath. Brown rhombic crystals were formed in 5−7 days. $Pr_4N^+CA^{-\bullet}$: A 100 mL flask equipped with a Schlenk adapter was charged with 21 mg (about 0.05 mmol) of $Pr_4N^+CA^{-\bullet}$, and 10 mL of dichloromethane was added under argon atmosphere. After dissolution, the solution was covered with hexane and put into a cold (−65 °C) bath. Orange crystals were formed during 3−5 days. The X-ray crystallographic analyses for DDQ and $Et_4N^+DDQ^{-\bullet}$ (data available in the literature) were remeasured at −150 °C to obtain better precision.

$(Et_4N^+)_2(DDQ_3)^{2-}$. Formula: $C_{40}H_{40}Cl_6N_8O_6$, M 941.50, monoclinic $P2_1/n$, $a = 13.084(1)$ Å, $b = 12.693(1)$ Å, $c = 13.656(1)$ Å, $\beta = 112.61(1)°$, $V = 2093.9(2)$ Å^3, $D_c = 1.493$ gcm^{-3}, $Z = 2$. The total number of reflections measured were 22997, of which 6779 reflections were symmetrically nonequivalent. Final residuals were R1 = 0.1061 and wR2 = 0.1995 for 5882 reflections with $I > 2\sigma(I)$.

$Pr_4N^+CA^{-\bullet}\cdot CH_2Cl_2$. Formula: $C_{19}H_{30}Cl_6NO_2$, M 517.14, monoclinic C_c, $a = 19.885(1)$ Å, $b = 7.8652(4)$ Å, $c = 18.427(1)$ Å, $\beta = 121.04(1)°$, $V = 2469.3$ (2) Å^3, $D_c = 1.391$ g cm^{-3}, $Z = 4$. The total number of reflections measured were 13363, of which 6949 reflections were symmetrically nonequivalent. Final residuals were R1 = 0.030 and wR2 = 0.0769 for 6689 reflections with $I > 2\sigma(I)$.

$Et_4N^+DDQ^{-\bullet}$. Formula: $C_{16}H_{20}Cl_2N_3O_2$, M 357.25, monoclinic $P2_1/n$, $a = 6.879(1)$ Å, $b = 20.031(2)$ Å, $c = 12.409(1)$ Å, $\beta = 99.84(1)°$, $V = 1684.6$ (3) Å^3, $D_c = 1.409$ g cm^{-3}, $Z = 4$. The total number of reflections measured were 16604, of which 5118 reflections were symmetrically nonequivalent. Final residuals were R1 = 0.0304 and wR2 = 0.0815 for 4745 reflections with $I > 2\sigma(I)$.

DDQ. Formula: $C_8Cl_2N_2O_2$, M 227.00, orthorhombic *Pbca*, $a = 16.464(1)$ Å, $b = 5.8609(2)$ Å, $c = 17.715(1)$ Å, $V = 1709.4$ (1) Å^3, $D_c = 1.764$ g cm^{-3}, $Z = 8$. The total number of reflections measured were 24307, of which 3849 reflections were symmetrically nonequivalent. Final residuals were R1 = 0.0358 and wR2 = 0.0956 for 3081 reflections with $I > 2\sigma(I)$.

Spectral Measurements. The absorption spectra were recorded on a HP 8453 diode-array spectrometer (UV−vis) and Varian Cary 500 spectrometer (UV−vis−NIR). Low-temperature studies were carried out with the aid of a low-temperature Dewar equipped with quartz windows for UV−vis measurements. All operations were performed with freshly prepared solution of anion-radical salts in an inert (argon) atmosphere with Teflon-capped cuvettes (0.1−1.0 cm) equipped with sidearms. Typically, 2−4 mL aliquots of the 2−4 mM solutions of anion-radical salts in acetonitrile were placed in a 1 cm cuvette, and the solid parent acceptor was added in increments. Alternatively, the anion-radical solution was added with the aid of a hypodermic syringe to the cuvette charged with the solid (parent) acceptor. The absorbance of new the NIR band at its maximum was measured at different concentrations of the neutral acceptor, and the data were evaluated with the aid of the Benesi−Hildebrand correlation. [The upper limit of the concentration of the neutral acceptor was limited by its solubility and varied from ∼15 mM for TCNQ to ∼0.7 M for TCNE. It should be also noted that although small amounts of the anion-radical dimers were present in the acetonitrile solutions, their concentrations (estimated spectrophotometrically based on the literature data[18]) were less than 1% relative to the concentration of anion radical, and therefore did not materially affect the calculations.] The Benesi−Hildebrand procedure

(45) Perrin, D. D.; Armarego, W. L.; Perrin, D. R. *Purification of Laboratory Chemicals*, 2nd ed.; Pergamon: New York, 1980.
(46) (a) Melby, L. R.; Harder, R. J.; Hertler, W. R.; Mahler, W.; Benson, R. E.; Mochel, W. E. *J. Am. Chem. Soc.* **1962**, *84*, 3374. (b) Webster, O. W.; Mahler, W.; Benson, R. E. *J. Am. Chem. Soc.* **1962**, *84*, 3678. (c) Torrey, H. A.; Hunter, W. H. *J. Am. Chem. Soc.* **1912**, *34*, 702.
(47) Sheldrick, G. M. *SHELXS-86, Program for Structure Solution*; University of Gottingen: Germany, 1986.

provided reliable results only if one reactant was present in great excess, and the complexation of the reactant (in deficit) was in the 20−80% range. (Such conditions were difficult to achieve for all the systems due to the relatively small formation constants and limited solubility.) Therefore, the formation constants and extinction coefficients were checked by treatment of the absorption data with the aid of the Drago procedure involving the construction of plots of K^{-1} with ϵ.[48] Additionally, the extinction coefficients and the formation constants were checked by the temperature dependencies of the NIR absorptions. The bandwidths $\Delta\nu_{CT}$ in Table 3 were obtained by Gaussian deconvolution of the NIR bands using Microcal Origin 6.0. To follow simultaneously the spectral changes observed in the UV−vis (anion radical) and NIR (π-mer), a 1 mm cuvette was used [owing to the high extinction coefficients of anion radicals in Table 1].

Acknowledgment. We thank D. Sun for synthesis of the chloranil anion-radical salts, the preparation of their crystals, and the spectroscopic study of $CA/CA^{-\bullet}$ systems, S. V. Lindeman for crystallographic assistance, and the R. A. Welch Foundation and the National Science Foundation for financial support.

Supporting Information Available: Structural data (bond lengths) of the acceptors and their anion radicals (Table S1) as well as the spectral characteristics of anion radicals and their π-mers measured with alkali-metal and tetrabutylammonium counterions in different solvents (Table S2). Spectral changes in the UV−vis and NIR region upon the addition of neutral acceptors to their anion radicals (Figure S1), comparison of the π-mer spectra in systems with different counterions (Figure S2), and the energy diagrams for electron transfer in $TCNE^{-\bullet}$/TCNE and $CA^{-\bullet}$/CA systems (Figure S3). This material is available free of charge via the Internet at http://pubs.acs.org.

JA0211611

(48) Drago, R. S. *Physical Methods in Chemistry*; W. B. Saunders Company: Philadelphia, 1977.